Improved probabilistic streamlines tractography by 2nd order integration over fibre orientation distributions

J-D. Tournier[1,2], F. Calamante[1,2], and A. Connelly[1,2]

[1]Brain Research Institute, Florey Neuroscience Institutes (Austin), Melbourne, Victoria, Australia, [2]Department of Medicine, University of Melbourne, Melbourne, Victoria, Australia

INTRODUCTION

The probabilistic streamlines [1] approach is one of the most promising methods to perform diffusion-weighted tractography. It takes into consideration the inherent noisy nature of DW data, extends naturally to allow fibre tracking through regions containing crossing fibres, and can be implemented to be relatively fast. However, current implementations of this algorithm work by stepping along an orientation derived from the fibre orientation distribution (FOD) at the current point only, and can hence be viewed as first order integration methods. Such methods are known to 'overshoot', and this effect has indeed previously been reported for the deterministic streamlines algorithm [2]. Higher order (Runge-Kutta) integration methods have been proposed to improve the quality of tracking results obtained using tensor-based deterministic streamlines [3], but unfortunately these are not suitable for probabilistic multi-fibre fibre-tracking applications. In this study, we propose a novel higher order probabilistic streamlines method, based on 2nd order integration over fibre orientation distributions (iFOD2).

METHODS

Current probabilistic streamlines algorithms (referred to herein as iFOD1) generally work by stepping along a particular direction by a fixed step-size, with a constraint on the angle between successive steps. The direction for each step is obtained by sampling the FOD at the current point, such that the probability of a particular direction being produced is proportional to the amplitude of the FOD along that direction. As illustrated in Figure 1 (left), in regions with high curvature, each step will on average cause the algorithm to overshoot, and the resulting tracks will tend to veer off course. This effect is demonstrated on simulated data in Figure 2. While this problem can be mitigated to some extent by reducing the step-size, this then makes it difficult to apply realistic priors on the curvature of the tracks. For example, a step size of 0.1mm combined with a maximum angle of 45º between successive steps corresponds to a radius of curvature of only approximately 0.25mm, thus allowing the algorithm to take paths that would not otherwise be considered realistic, as demonstrated in Figure 3 (left). Note that this problem is avoided in practice by lowering the maximum angle between successive steps, but this again causes the algorithm to overshoot in regions of high curvature (data not shown).

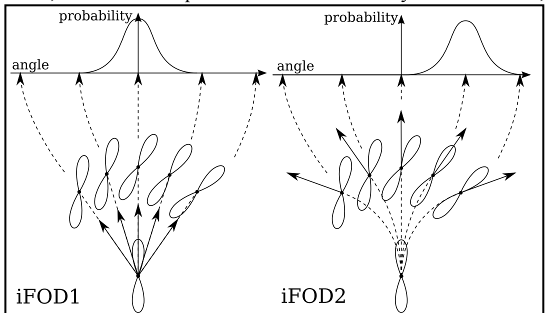

Figure 1: illustration of the 2nd order probabilistic integration concept. In both cases, the FOD at the current point is shown at the bottom, along with the FODs at a number of candidate points for the next step. Left: with first-order methods (iFOD1) only the FOD at the current point is considered; in this example, the path with highest probability would be directly forward. Right: with iFOD2, the FOD at each point along each candidate path is taken into account; in this case the curve with highest *joint* probability corresponds to the most likely path.

The proposed iFOD2 algorithm is illustrated in Figure 1 (right). Rather than stepping along straight-line segments, the algorithm steps along a path given by an arc of a circle of fixed length (the step-size), tangent to the current direction of tracking at the current point. As for iFOD1, the actual path selected for each step is obtained by sampling a probability density function (PDF), but rather than sampling from the local FOD only, in iFOD2 the probability of each path is calculated as the product of the probabilities of each infinitesimal step making up that path. This probability is approximated by computing the product of the amplitude of the FOD, evaluated at regular intervals (4 in this study) along the tangent to the path. This PDF is illustrated in Figure 1, showing the probability of each path as a function of the orientation of its tangent at the end point. As can be appreciated, with iFOD2 the most probable path corresponds to the expected curve through that region. In contrast, with iFOD1 the most probable step would be directly forward (Figure 1, left).

The PDF used in iFOD2 can be sampled relatively easily. For each step, each possible path is parameterised by the orientation of the tangent at its end point (i.e. one step-size along the path), leading to a low-dimensional 2D PDF. Furthermore, the curvature constraint imposes a maximum value on the angle between the tangents at the end points. Sampling this PDF is therefore a problem of similar complexity to the iFOD1 case, since it reduces to producing an independent sample from a PDF defined over orientations within a predefined range. This was achieved with good efficiency using the simple rejection sampling algorithm [4].

For both iFOD implementations, the FOD at the current point was evaluated using tri-linear interpolation from the 8 nearest neighbours. For the real data, FODs were estimated using Constrained Spherical Deconvolution [5] as implemented in MRtrix [6] (with l_{max}=10), and tracks were terminated when the FOD amplitude fell below a user-defined threshold of 0.1.

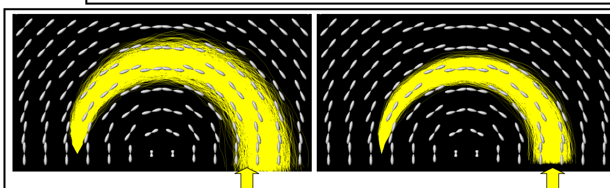

Figure 2: 1000 probabilistic streamlines launched from a single seed point over a simulated curved data set. Left: with iFOD1, the tracks tend to overshoot by a considerable distance (correct end point shown by the arrow). Right: with iFOD2, the tracks tend to follow the true curve correctly. The step-size was 1mm in both cases.

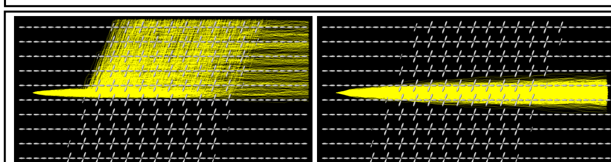

Figure 3: 1000 probabilistic streamlines launched from a single seed point over a simulated 70º crossing data set. Left: with iFOD1 (step-size 0.2mm), many of the tracks veer off course. Right: with iFOD2 (step-size 1mm), all tracks follow the left-right orientation correctly.

RESULTS

The ability of iFOD2 to track through highly curved regions is demonstrated in Figure 2. As can be appreciated, with all other parameters being equal, iFOD2 shows no bias, whereas iFOD1 demonstrates a clear overshoot. This effect can be minimised by reducing the step-size (not shown), however this does allow iFOD1 to take unrealistic paths, as shown in Figure 3 (left). In contrast, iFOD2 tracks correctly through this region of crossing fibres (using the same step size as in Figure 2).

Figure 4 shows tracks produced using iFOD2 from real data, acquired on a 3T Siemens Trio (150 DW directions, b = 3000 s/mm^2, 2.3mm cubic voxels). Tracks were seeded from 100,000 points placed at random throughout the whole brain. As can be appreciated, the results correspond well with the known anatomy. Note in particular the excellent delineation of the highly curved subcortical U-fibres and the extensive crossing fibres in the centrum semiovale.

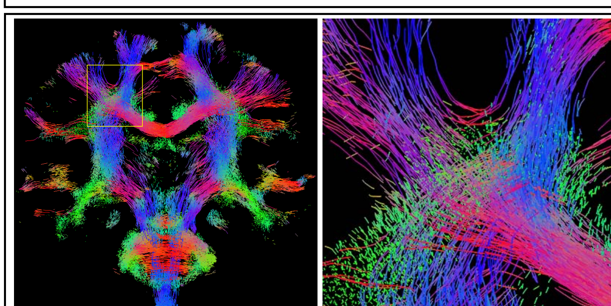

Figure 4: whole-brain results obtained by launching from 100,000 seed points placed randomly throughout the brain, shown as a 1mm thick coronal projection. Tracks are colour-coded according to their local orientation (red: left-right; green: anterior-posterior; blue: inferior-superior). Right: a close-up of the region highlighted on the left, showing an excellent delineation of the subcortical U-fibres, as well as fibres crossing extensively throughout the region.

DISCUSSION

By making use of a 2nd order strategy, the proposed iFOD2 algorithm is capable of tracking with high accuracy though both highly-curved and crossing-fibre regions, using a relatively large step-size. Moreover, the use of a step-size similar to the voxel dimensions permits the use of a realistic prior on curvature, further reducing the incidence of unrealistic tracks.

REFERENCES: [1] Behrens et al., MRM 50:1077-88 (2003). [2] Tournier et al., MRM 47:701-8 (2002). [3] Basser et al., 44:625-32 (2000). [4] Mackay, "Information Theory, Inference, and Learning Algorithms", Cambridge Univ. Press, p365-5 (2003). [5] Tournier et al., NeuroImage 35:1459-72 (2007). [6] MRtrix, http://www.brain.org.au/software/.